Available online at www.sciencedirect.com
ScienceDirect
Journal of Molecular Catalysis A: Chemical 256 (2006) 247–255
JOURNAL OF MOLECULAR CATALYSIS A: CHEMICAL
www.elsevier.com/locate/molcata

Direct oxidation of benzene to phenol by molecular oxygen over catalytic systems containing $Pd(OAc)_2$ and heteropolyacid immobilized on HMS or PIM

Yanyong Liu *, Kazuhisa Murata, Megumu Inaba

Biomass Technology Research Center, National Institute of Advanced Industrial Science and Technology (AIST), AIST Tsukuba Central 5, 1-1-1 Higashi, Tsukuba, Ibaraki 305-8565, Japan

Received 24 January 2006; received in revised form 1 May 2006; accepted 4 May 2006
Available online 6 June 2006

Abstract

Heteropolyacid (HPA) and $Pd(OAc)_2$ were immobilized through chemical bonds onto the functional organic groups modified solid surfaces of hexagaonal mesoporous silica (HMS) and polyimine (PIM). The obtained hybrid samples were used as heterogeneous catalysts for the oxidation of benzene to phenol by molecular oxygen and compared to the homogeneous catalytic system containing HPA and $Pd(OAc)_2$ (denoted by HPA + $Pd(OAc)_2$). The activity of various catalytic systems was in the order of HPA + $Pd(OAc)_2$ > HMS–HPA + $Pd(OAc)_2$ > PIM–HPA + $Pd(OAc)_2$ > HPA + HMS–$Pd(OAc)_2$ > HMS–HPA + HMS–Pd(OAc). Although the benzene conversions over the heterogeneous catalytic systems containing solid catalysts were lower than that over the homogeneous catalytic system HPA + $Pd(OAc)_2$, HMS–HPA + $Pd(OAc)_2$ gave the same maximum achievable yield of phenol as that over HPA + $Pd(OAc)_2$ by extending the reaction time or increasing the catalyst amount. Moreover, HMS–HPA + $Pd(OAc)_2$ was able to be reused after simple filtration without leaching HPA. The benzene conversion and the selectivity to phenol over the heterogeneous system HMS–HPA + $Pd(OAc)_2$ did not decrease even after reused five times.

Keywords: Benzene oxidation; Phenol; Heteropolyacid; Palladium acetate; HMS; PIM; Surface modification; Molecular oxygen

1. Introduction

Phenol is one of the most important chemicals in the fields of resin, fiber and medicine manufacture. The current worldwide capacity for phenol production is nearly 7 million metric tonnes/year. More than 90% phenol have been produced by the cumene process, which is a three-step process and coproduces acetone in the molar ratio of 1:1 with respect to phenol. The economical efficiency of the cumene process is strongly dependent on the market price of acetone. Many efforts are in progress for the development of a one-step process for phenol synthesis by the direct oxidation of benzene [1]. Although H_2O_2 and N_2O can directly oxidize benzene to phenol in high selectivity [2,3], H_2O_2 and N_2O are currently too expensive to allow an economically viable process. Molecular oxygen (O_2) is the best oxidant due to low cost and significant advantages to the environment. Although high selectivity to phenol could be obtained in the benzene oxidation by O_2 in the presence of a reducing agent (such as H_2, CO, NH_3, dithioalcohols, ascorbic acid, etc.) [4–8], the direct oxidation of benzene to phenol by O_2 without any reducing regents would be of great value in industry.

Heteropolyacid (HPA) catalysts are very attractive since they have both strong acidity and redox properties, and the two important properties for catalysis can be controlled through choosing appropriate constituent elements [9,10]. These merits make them potentially useful for the selective oxidation of hydrocarbons. A homogeneous catalytic system containing heteropolyacid and $Pd(OAc)_2$ (denoted by HPA + $Pd(OAc)_2$) has been reported to be effective for the direct oxidation of benzene to phenol by O_2 [11,12]. From the point of view of green chemistry, heterogeneous catalysts are desirable in the industrial manufacture because of their versatility, ease of separation, no corrosiveness, long lifetime and regenerability. In order to improve the homogeneous catalytic system HPA + $Pd(OAc)_2$, heteropolyacid was encapsulated in MCM-41 and VPI-5 for the direct oxidation of benzene by O_2 in the presence of $Pd(OAc)_2$ [13]. How-

* Corresponding author. Tel.: +81 29 861 4774; fax: +81 29 861 4774.
E-mail address: yy.ryuu@aist.go.jp (Y. Liu).

1381-1169/$ – see front matter © 2006 Elsevier B.V. All rights reserved.
doi:10.1016/j.molcata.2006.05.015

ever, these attempts were unsuccessful because heteropolyacid leached from MCM-41 and the reactants were difficult to enter into the relatively small pores of VPI-5 [13].

There are several excellent methods for immobilizing heteropolyanions on the solid surfaces without leaching into reaction solvent during reaction for the heterogeneous catalysis, such as the formation of insoluble solid salts (such as Cs salt) [14], the intercalation of heteropolyanions into anion-exchange materials (such as hydrotalcites) [15] and the anchorage of heteropolyanions onto the functional organic groups modified solid surfaces [16–18]. The process of anchoring heteropolyanions onto the functional organic groups modified solid surfaces includes two steps as follows: first, organic amino groups were grafted on the solid surfaces; then heteropolyanions were immobilized on the solid surfaces using an acid–base reaction between heteropolyacid and the grafted organic amino groups. Organic amino group modified silica [16,17] and polyimine (PIM) [18] are usually used as the supports for anchoring heteropolyanions. Recently, we have successfully anchored peroxo-heteropoly anions on the surface of Pd exchanged HMS as a heterogeneous catalyst [19] to improve the homogeneous system containing $Pd(OAc)_2$ and peroxo-heteropoly compounds for the propylene epoxidation by O_2 in methanol [20]. In the meantime, $Pd(OAc)_2$ could also be immobilized on the silica surface through reacting with the functional organic ligands grafted on the silica surface [21,22]. The active species in these hybrid catalysts hardly leach from supports into solvent during the reaction because they are fixed on the solid support surfaces through chemical bonds.

In this study, we immobilized heterpolyacid and $Pd(OAc)_2$ on the surface of hexagonal mesoporous silica (HMS) and polyimine using the surface modification method. The obtained solid samples were used as heterogeneous catalysts for the direct oxidation of benzene to phenol by O_2 and compared to the homogeneous catalytic system containing heteropolyacid and $Pd(OAc)_2$.

2. Experimental

2.1. Catalyst preparation

Molybdovanadophosphoric acids ($H_{3+x}[PMo_{12-x}V_xO_{40}]$ ($x = 0$–3)) were prepared using the procedure of Tsigdinos and Hallada [23] and the products were confirmed by FT-IT spectra and elemental analyses. $H_3[PMo_{12}O_{40}]$, $H_4[PMo_{11}VO_{40}]$, $H_5[PMo_{10}V_2O_{40}]$ and $H_6[PMo_9V_3O_{40}]$ were denoted by HPA(V0), HPA(V1), HPA(V2) and HPA(V3), respectively.

Aminopropyl group-modified HMS (denoted by HMS–$PrNH_2$) was prepared according to the method reported in Refs. [24,25]. Tetraethoxysilane (TEOS, 18.5 g, 0.09 mol) and 3-aminopropyl-trimethoxysilane (AMPS, 1.79 g, 0.01 mol) were added, separately, to a stirred mixture of ethanol (41 g), distilled water (53 g) and *n*-dodecylamine (5.09 g) at room temperature. After 10 min the turbid solution became milky, and stirring was continued for 18 h, yielding a thick white suspension. The solid product was filtered and dried at room temperature. The template *n*-dodecylamine was removed by heating the solid (ca. 2 g) at reflux in absolute ethanol (100 ml) for 3 h, and this operation was repeated three times.

HMS–$PrNH_2$ bonded HPA (denoted by HMS–HPA) was prepared using a method similar to that for preparing MCM-41-$PrNH_2$ bonded HPA [16]. HMS–$PrNH_2$ (1 g) was treated with 60 ml of refluxing methanol solution containing 5% HPA for 3 h. Then the solid product was filtered, washed and dried at 323 K in a vacuum for 12 h.

Polyimine bonded HPA (denoted by PIM–HPA) was prepared using the method reported in Ref. [19]. PIM support was prepared from *p*-phenylenediamine (5.4 g) and terephthaldehyde (6.7 g) in a solution of 10 g of anhydrous sodium acetate in 35 ml of glacial acetic acid. The bonding HPA to the base form of PIM was carried out at room temperature in 0.02 M acetonitrile solution for 5 h (the molar ratio of PIM to HPA was 1:0.25). Then the solid product was filtered, washed and dried at 323 K in a vacuum for 12 h.

HMS bonded $Pd(OAc)_2$ (denoted by HMS-Pd) was prepared using a method similar to that for preparing SiO_2 bonded $Pd(OAc)_2$ [19]. First, HMS–$PrNH_2$ (5 g) was allowed to react with 2-acetylpyridine (0.6 g) in 100 ml absolute ethanol at 333 K for 24 h to graft the functional organic ligand on the HMS surface. Then the obtained modified-HMS (4 g) and $Pd(OAc)_2$ (0.1 g) were stirred in 100 ml acetone at room temperature for 24 h. The solid product was filtered, washed and dried at 323 K in a vacuum for 12 h.

Supported catalyst HPA/HMS was prepared as a reference using a wet impregnation method. Calcined HMS powder was stirred in heteropolyacid aqueous solution at 323 K. After evaporation of water at 323 K, the solid product was filtered and dried at 323 K in a vacuum for 12 h.

2.2. Instruments

Elemental analysis was carried out using a Thermo Jarrell Ash IRIS/AP instrument. Fourier transform infrared (FT-IR) spectra were recorded by a JASCO FT/IR 7000 spectrometer using KBr pellets under atmospheric conditions. Power X-ray diffraction (XRD) patterns were measured using a MAC Science MXP-18 diffractometer with Cu Kα radiation operated at 40 kV and 50 mA. UV–vis diffuse reflectance (DR-UV–vis) spectra were recorded on a JASCO-550 spectrophotometer at room temperature. Scanning electron microscope (SEM) observation was carried out using a JEOL JSM-5600/LV system. N_2 adsorption isotherms were measured at 77 K using a Belsorp 28SA automatic adsorption instrument. The samples were dried at 573 K for 8 h before the measurement. The surface area of each sample was obtained from a Brunanuer–Emmett–Teller (BET) plot.

2.3. Catalytic reaction

The oxidation of benzene was carried out in a 50 ml teflon-coated autoclave, which was immersed into an oil-bath. In a typical experiment, a certain amount of catalyst and 0.2 g LiOAc were added into a mixed liquid containing 2 ml acetic acid, 4 ml water, 2 ml sulfolane and 2 ml benzene. After 2.0 M PaO_2 was charged to the autoclave at 298 K, the oxidation reaction was

conducted at 393 K with vigorous stirring. After reaction, the gas phase was analyzed by a TCD gas chromatograph kept at 373 K using a Porapak Q column (3 m) and a molecular sieve 5A column (3 m). The liquid phase was analyzed using a Shimadzu LC-10AD HPLC. A methanol/water gradient, starting at 60/40 (v/v) and reaching 100% methanol in 10 min was used for elution. The samples were prepared by dissolution in methanol/water (60/40, v/v). The products were quantified using calibration curves. The UV–vis spectra of the products were recorded and compared with those of authentic samples. The identification of the reaction products was carried out by GC-MS.

3. Results and discussion

3.1. Characterization of various samples

$[PMo_{12-x}V_xO_{40}]^{-3-x}$ ($x = 0$–3) heteropolyanions used in this study possess the Keggin structure, which are the most popular heteropolyanions used in catalysis [9,10]. As shown in Fig. 1, a Keggin type heteropoly anion consists of a central XO_4 tetrahedron (X = P^{5+}, Si^{4+}, Ge^{4+}, etc.) surrounded by 12 octahedra MO_6 (M = W^{6+}, Mo^{6+}, V^{5+}, etc.). The 12 MO_6 octahedra comprise four groups of three edge-shared octhedra, the M_3O_{13} triplet, which have a common oxygen vertex connected to the central XO_4 tetrahedron. Thus, the oxygen atoms in this structure fall into four classes of symmetry-equivalent oxygen atoms: X–O_a; M–O_b–M, connecting two M_3O_{13} units by corner sharing; M–O_c–M, connecting two M_3O_{13} units by edge sharing; and M–O_d [26].

The infrared spectra of various samples are shown in Fig. 2. As for $H_5PMo_{10}V_2O_{40}$, the peak at 1080 cm^{-1} is assigned to the asymmetric stretching of P–O_a, the peak at 970 cm^{-1} is assigned to the vibration of M–O_d (M = Mo, V), the peak at 870 cm^{-1} is assigned to the vibration of M–O_b–M (M = Mo, V), and the peak at 790 cm^{-1} is assigned to the vibration of M–O_c–M (M = Mo, V). As for HMS–$PrNH_2$, the peak at around 1090 cm^{-1} and its shoulder are assigned to the asymmetric stretching of Si–O–Si, and the peak at around 810 cm^{-1} is given by the vibration of "internal" bands in SiO_4^{4-} tetrahedra. On the other hand, PIM showed its characteristic CH=N vibrations and the para-substituted aromatic ring vibrations in the IR spectrum. As for the hybrid samples, HMS–HPA(V2) showed all peaks of $H_5PMo_{10}V_2O_{40}$ and HMS–$PrNH_2$, and PIM–HPA(V2) showed all peaks of $H_5PMo_{10}V_2O_{40}$ and PIM with a little shift in the IR spectra. These results indicate that $H_5PMo_{10}V_2O_{40}$ was successfully immobilized on the solid supports (HMS–$PrNH_2$ and PIM) without collapse during the immobilization process.

The X-ray diffraction patterns of various samples are shown in Fig. 3. HMS–$PrNH_2$ exhibited a strong (1 0 0) reflection at about 2.3° corresponding to $d \approx 4$ nm. Moreover, hexagonal order weak (1 1 0) and (2 0 0) reflections were also observed in the 2θ ranged from 4.0° to 6.0°. The weak and broad peak at about 22° was observed due to the existence of a small amount of amorphous SiO_2 in HMS–$PrNH_2$. The XRD pattern of HMS–$Pd(OAc)_2$ was quite similar to that of HMS–$PrNH_2$, which indicates that the pore structure of HMS hardly changed after introducing $Pd(OAc)_2$ molecules onto the organic ligands on the HMS surface. On the other hand, $H_5PMo_{10}V_2O_{40}$ showed its characteristic reflections from 8.0° to 70.0° in the XRD pattern. As for the XRD pattern of HMS–HPA(V2), the strong (1 0 0) reflection of HMS–$PrNH_2$ greatly decreased and a broad band at around 6° appeared after introducing $H_5PMo_{10}V_2O_{40}$ onto the amino groups on the HMS surface. These results indicate that the mesoporous structure of HMS–$PrNH_2$ greatly reduced after $H_5PMo_{10}V_2O_{40}$ molecules were bonded on the surface of HMS–$PrNH_2$. However, because the peaks of $H_5PMo_{10}V_2O_{40}$ particles cannot be observed in the XRD pattern of HMS–HPA(V2), $H_5PMo_{10}V_2O_{40}$ molecules

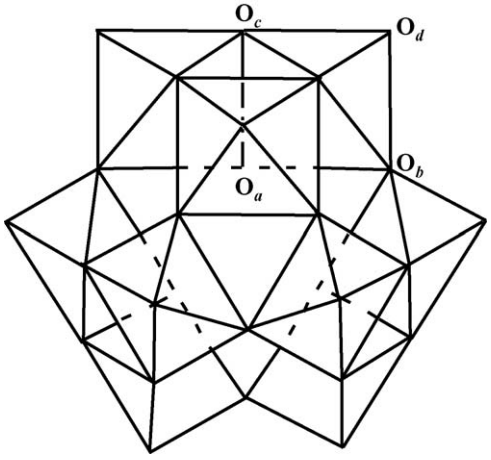

Fig. 1. Structure of Keggin type heteropoly anion $[PMo_{12-x}V_xO_{40}]^{-3-x}$.

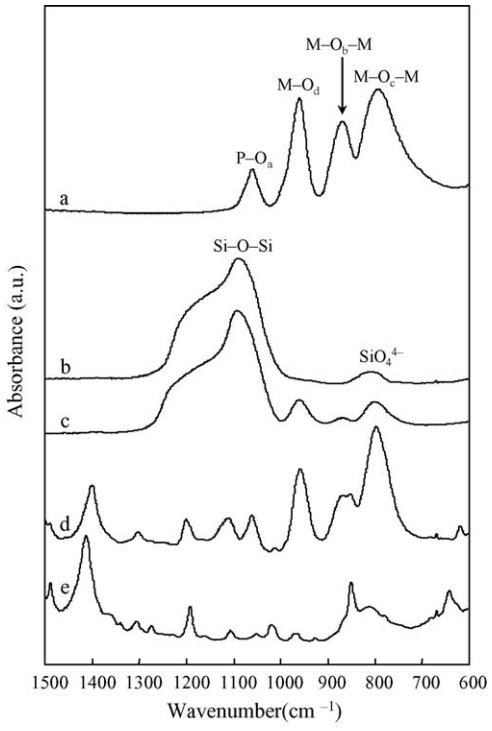

Fig. 2. FT-IR spectra of various samples: (a) $H_5PMo_{10}V_2O_{40}$ (HPA(V2)); (b) HMS–$PrNH_2$; (c) HMS–HPA(V2); (d) PIM–HPA(V2); (e) PIM.

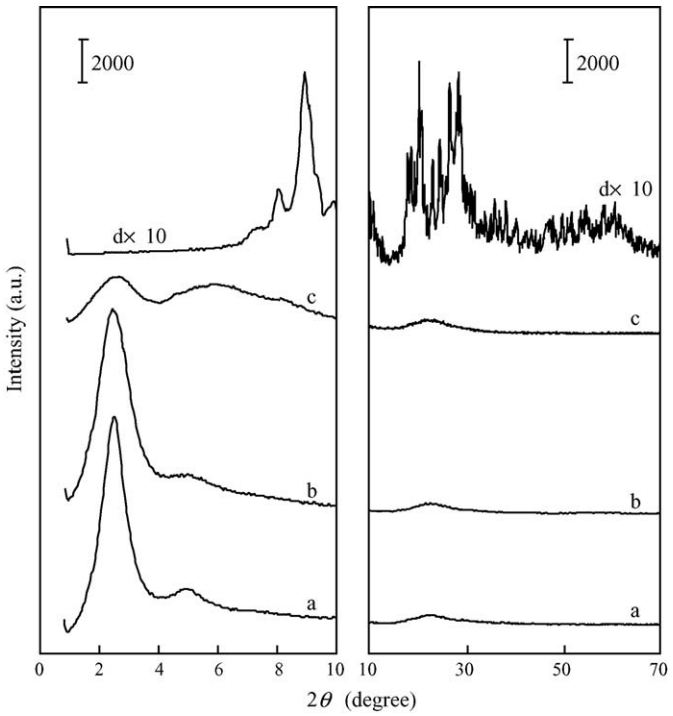

Fig. 3. XRD patterns of various samples: (a) HMS–$PrNH_2$; (b) HMS–$Pd(OAc)_2$; (c) HMS–HPA(V2); (d) $H_5PMo_{10}V_2O_{40}$ (HPA(V2)).

in HMS–HPA(V2) are uniformly distributed on the surface of HMS–$PrNH_2$.

The N_2 adsorption–desorption isotherms of various samples are shown in Fig. 4. The hysteresis loop of HMS–$PrNH_2$ was close to the H1 type according to IUPAC classification [27]. The abrupt step appeared in the region of $P/P_0 = 0.3$–0.4, which implied the existence of uniform mesopores in HMS–$PrNH_2$. The N_2 adsorption–desorption isotherms of HMS–$Pd(OAc)_2$

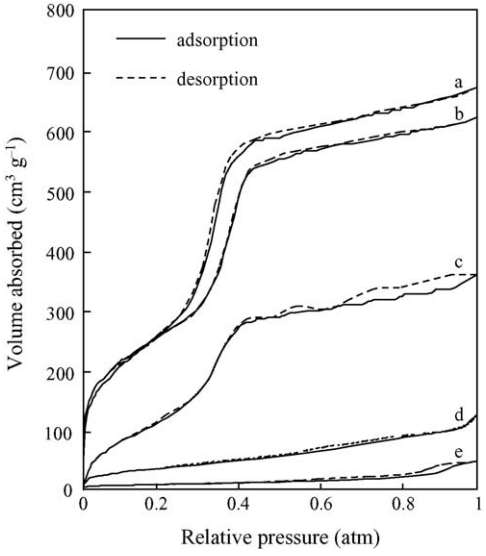

Fig. 4. N_2 adsorption–desorption isotherms of various samples: (a) HMS–$PrNH_2$; (b) HMS–$Pd(OAc)_2$; (c) HMS–HPA(V2); (d) PIM–HPA(V2); (e) $H_5PMo_{10}V_2O_{40}$ (HPA(V2)).

were quite similar to those of HMS–$PrNH_2$ but the N_2 absorbed volume decreased slightly, which indicates that the mesoporous structure was almost retained and the BET surface area slightly decreased after $Pd(OAc)_2$ molecules were bonded onto the organic ligand on the HMS surface. On the other hand, in the N_2 adsorption–desorption isotherms of HMS–HPA(V2), both the abrupt step in the region of $P/P_0 = 0.3$–0.4 and the N_2 absorbed volume greatly decreased compared to those of HMS–$PrNH_2$. These results indicate that the pore system deteriorated in HMS–HPA(V2) after $H_5PMo_{10}V_2O_{40}$ molecules were bonded onto the amino groups on the HMS surface. However, the hysteresis loop of HMS(V2) was also close to the H1 type, implying that the meseporous structure still remained to some extent. As for PIM–HPA(V2) and $H_5PMo_{10}V_2O_{40}$, their hysteresis loops in the N_2 adsorption–desorption isotherms were close to the H2 type, indicating that there is no porous structure in these samples.

Fig. 5 shows the SEM pictures of $H_5PMo_{10}V_2O_{40}$, HMS–$PrNH_2$, HMS–HPA(V2) and HMS–$PrNH_2$ + HPA(V2) (physical mixture of HMS–$PrNH_2$ and HPA(V2)) at the same magnification. $H_5PMo_{10}V_2O_{40}$ consists of agglomerated crystallites, while HMS–$PrNH_2$ consists of small amorphous particles. As for the physical mixture HMS–$PrNH_2$ + HPA(V2), small amorphous particles of HMS–$PrNH_2$ were observed on the surface of the large crystallites of $H_5PMo_{10}V_2O_{40}$. On the other hand, the hybrid sample HMS–HPA(V2) prepared by immobilizing $H_5PMo_{10}V_2O_{40}$ on the surface of HMS–$PrNH_2$ through chemical bonds showed a SEM picture highly similar to that of the HMS–$PrNH_2$ support. No typical separated crystallites of unsupported $H_5PMo_{10}V_2O_{40}$ phase could be found in the SEM photograph of HMS–HPA(V2) although the loading of HPA(V2) was about 30 wt% in HMS–HPA(V2). These results indicate that $H_5PMo_{10}V_2O_{40}$ molecules were uniformly dispersed on the HMS surface in HMS–HPA(V2), coinciding with the results obtained from XRD patterns.

The physical properties of various samples are shown in Table 1. HMS–$PrNH_2$ possesses a large BET surface area of $1030\ m^2\ g^{-1}$. After $Pd(OAc)_2$ molecules were bonded onto the organic functional groups grafted on the HMS surface, the BET surface area slightly decreased because the loading amount of $Pd(OAc)_2$ in HMS–$Pd(OAc)_2$ was low (2 wt%). On

Table 1
Physical properties of various samples

Sample	BET surfure area ($m^2\ g^{-1}$)	Loading (wt%)[a]	P:Mo:V (molar ratio)[a]
HMS–$PrNH_2$	1030	–	–
HMS–$Pd(OAc)_2$	996	2[b]	–
HMS–HPA(V0)	451	44[c]	1:12.0:0
HMS–HPA(V1)	467	36[c]	1:10.9:1.1
HMS–HPA(V2)	485	30[c]	1:10.0:2.1
HMS–HPA(V3)	516	25[c]	1:8.9:3.1
PIM	48	–	–
PIM–HPA(V2)	31	28[c]	1:9.9:2.0

[a] Obtained by ICP analyses.
[b] Loading amount of Pd(OAc).
[c] Loading amount of HPA.

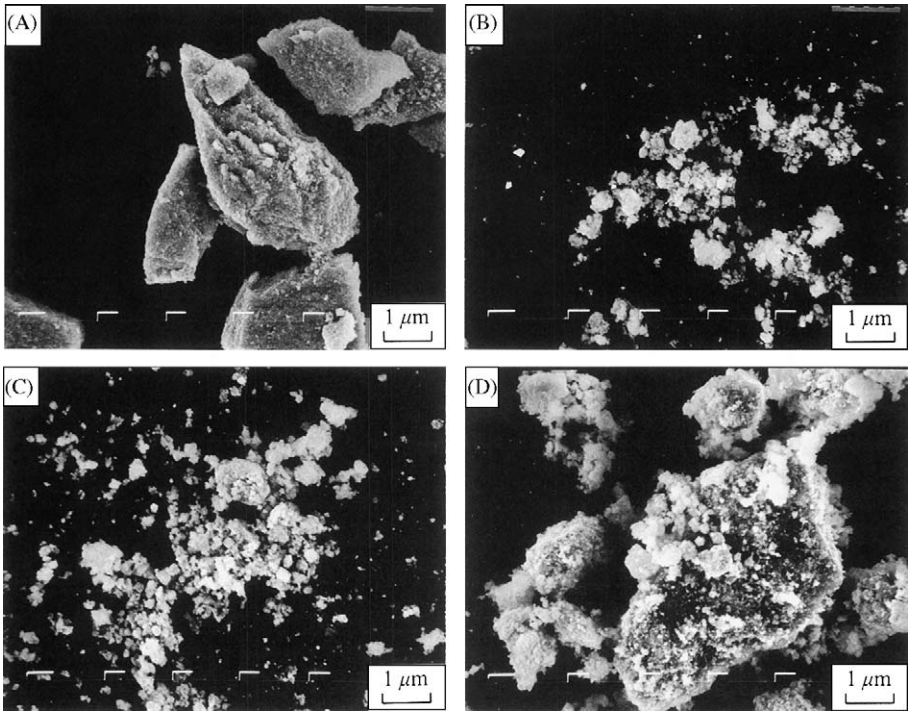

Fig. 5. SEM micrographs of various samples: (A) $H_5PMo_{10}V_2O_{40}$ (HPA(V2); (B) HMS–$PrNH_2$; (C) HMS–HPA(V2); (D) HMS–$PrNH_2$ + (HPA(V2) (physical mixture).

the other hand, the loading amount of HPA immobilized onto HMS–$PrNH_2$ was over 25 wt% for each HMS–HPA sample, which caused the severe decreases in BET surface areas after immobilizing heteropolyanions on HMS–$PrNH_2$. The blocking of mesopores in HMS–$PrNH_2$ by heteropolyanions and/or the partly collapse of the walls of mesopores in HMS–$PrNH_2$ caused the decrease in the BET surface area of the hybrid samples HMS–HPA. Even so, all HMS–HPA samples prepared in this study still showed BET surface areas above 450 $m^2\ g^{-1}$, which is much higher than those of silica anchored heteropolyanion samples. On the other hand, PIM–HPA(V2) showed a low BET surface area of 31 $m^2\ g^{-1}$ due to the low BET surface area of the non-porous PIM support (48 $m^2\ g^{-1}$). We synthesized the HMS–$Pd(OAc)_2$ sample using the reaction of 4 g modified-HMS with 0.1 g $Pd(OAc)_2$ (shown in Section 2) according to Ref. [24]. Thus, the designed $Pd(OAc)_2$ loading in the HMS–$Pd(OAc)_2$ sample was 2.5 wt%. Using ICP elemental analyses, we knew that the actual $Pd(OAc)_2$ loading in the HMS–$Pd(OAc)_2$ sample was about 2 wt%. The loading amounts of heteropolyanions in HMS–HPA samples were affected by the charge balance between the grafted $PrNH_2$ groups and heteropolyanions. The negative charges are 3, 4, 5 and 6 for $[PMo_{12}O_{40}]$, $[PMo_{11}VO_{40}]$, $[PMo_{10}V_2O_{40}]$ and $[PMo_9V_3O_{40}]$, respectively, resulting in the loading amount of heteropolyanion in HPA–HMS samples in the order of HMS–HPA(V0) > HMS–HPA(V1) > HMS–HPA(V2) > HMS–HPA(V3). In the meantime, the larger loading amount of $[PMo_{12}O_{40}]$ caused the lower BET surface area of HMS–HPA(V0). The P/Mo/V molar ratio estimated from ICP elemental analyses was very close to that in the formula for each HPA-containing sample, indicating that heteropolyanions

Table 2
Benzene oxidation with O_2 over various catalytic system at 393 K[a]

Catalytic system	Catalyst amount (g)	Reaction time (h)	Benzene conversion (%)	Selectivity to phenol (%)	Turnover number
HPA(V2) + $Pd(OAc)_2$	0.15 + 0.01[b]	6	12.6	74.8	63.8
HMS–HPA(V2) + $Pd(OAc)_2$	0.5 + 0.01[c]	6	8.1	81.4	41.0
	0.5 + 0.01[c]	10	12.2	75.6	61.8
PIM–HPA(V2) + $Pd(OAc)_2$	0.5 + 0.01[c]	10	6.7	73.2	33.9
HPA(V2) + HMS–$Pd(OAc)_2$	0.15 + 0.5[d]	10	4.8	70.3	24.3
HMS–HPA(V2) + HMS–$Pd(OAc)_2$	0.5 + 0.5[e]	10	1.2	60.2	6.1

[a] Autoclave, 50 ml; HOAc, 2 ml; sulfolane, 2 ml; H_2O, 4 ml; benzene, 2 ml; LiOAc, 0.2 g. O_2, 2.0 MPa.
[b] HPA(V2), 0.15 g; $Pd(OAc)_2$, 0.01 g.
[c] HMS–HPA(V2) or PIM–HPA(V2), 0.5 g; $Pd(OAc)_2$, 0.01 g.
[d] HPA(V2), 0.15 g; HMS–$Pd(OAc)_2$, 0.5 g.
[e] HMS–HPA(V2), 0.5 g; HMS–$Pd(OAc)_2$, 0.5 g.

did not collapse after anchoring on the surface of HMS and PIM supports.

3.2. Oxidation of benzene to phenol by molecular oxygen

The results of the benzene oxidation by O_2 at 393 K over various catalytic systems are shown in Table 2. We used proper amounts of $Pd(OAc)_2$ (0.01 g) and HPA (0.15 g) in the homogeneous system for the benzene oxidation according to the results reported in Refs. [11,12]. We used almost the same amounts of $Pd(OAc)_2$ and HPA in the solid catalysts as those used in the homogeneous system. Because the loading amount of $Pd(OAc)_2$ was about 2 wt% in HMS–$Pd(OAc)_2$ and the loading amounts of $H_5PMo_{10}V_2O_{40}$ were about 30 wt% in HMS–HPA(V2) and PIM–HPA(V2) (Table 1), all catalytic systems listed in Table 2 contained almost the same amounts of $Pd(OAc)_2$ (0.01 g) and HPA (0.15 g). The selectivity to phenol over each catalytic system was over 70% except the dual solid system HMS–HPA(V2) + HMS–$Pd(OAc)_2$ (60.2%) for benzene oxidation by O_2 at 393 K for 6 h. The byproducts observed were catechol, hydroquinone, 1,4-benzoquinone, biphenyl and a very small amount of CO_2. The homogeneous catalytic system HPA(V2) + $Pd(OAc)_2$ showed a relatively high benzene conversion of 12.6% after 6 h. Among the catalytic systems containing solid catalysts, HMS–HPA(V2) + $Pd(OAc)_2$ system showed the highest benzene conversion (8.1%). The conversion and the selectivity to phenol over the heterogeneous system HMS–HPA(V2) + $Pd(OAc)_2$ after 10 h were quite similar to those over the homogeneous system HPA(V2) + $Pd(OAc)_2$ after 6 h. PIM–HPA(V2) + $Pd(OAc)_2$ catalytic system showed a lower conversion (6.7%) than that over HMS–HPA(V2) + $Pd(OAc)_2$ catalytic system (12.2%) after 10 h, which probably is due to the low surface area of PIM support (Table 1). In the meantime, HPA(V2) + HMS–$Pd(OAc)_2$ also showed a lower conversion (4.8%) than HMS–HPA(V2) + $Pd(OAc)_2$ (12.2%) after 10 h, implying that immobilizing HPA is more effective than immobilizing $Pd(OAc)_2$. On the other hand, the dual solid system consisting of HMS–HPA(V2) and HMS–$Pd(OAc)_2$ showed a very low conversion, which indicates that it is difficult to completely replace the homogeneous catalytic system with solid catalysts for the liquid-phase oxidation of benzene by O_2.

The plots of the phenol yields versus the benzene conversions over the homogeneous catalytic system HPA(V2) + $Pd(OAc)_2$ and the heterogeneous catalytic system HMS–HPA(V2) + $Pd(OAc)_2$ for the benzene oxidation by O_2 at 393 K are shown in Fig. 6; various phenol yields and benzene conversions were obtained by changing the reaction time or changing the catalyst amount. With increasing benzene conversion, the selectivity to phenol decreased mainly due to the further oxidation of phenol. Thus, the phenol yield has a maximum value. As shown in Fig. 6, the plots of the both systems are almost overlapped with each other. Both of them showed the highest phenol yields of about 16%. In other words, by increasing the catalyst amount or extending the reaction time, the heterogeneous system HMS–HPA(V2) + $Pd(OAc)_2$ gave the same conversion and the same selectivity to phenol as those obtained in the homogeneous system HPA(V2) + $Pd(OAc)_2$.

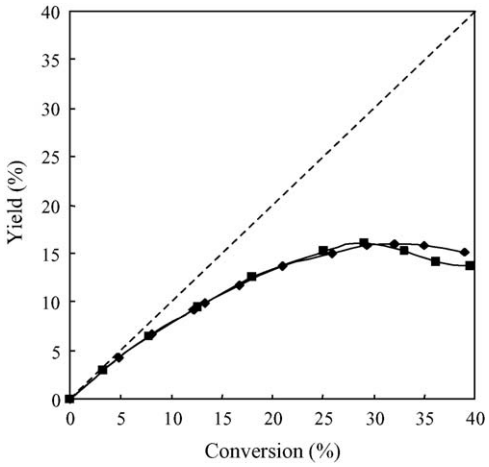

Fig. 6. Plots of phenol yield vs. benzene conversion for the oxidation of benzene by O_2 at 393 K. (■): homogeneous system HPA(V2) + $Pd(OAc)_2$; (♦): heterogeneous system HMS–HPA(V2) + $Pd(OAc)_2$. Autoclave, 50 ml; benzene, 2 ml; HOAc, 2 ml; H_2O, 4 ml; sulfolane, 2 ml; LiOAc, 0.2 g; O_2, 2.0 MPa.

The DR-UV–vis spectra of various samples are shown in Fig. 7. $H_5PMo_{10}V_2O_{40}$ showed the characteristic absorption bands of Keggin type heteropolyanions at about 210 and 260 nm corresponding to charge transfers of O_d–W^{VI} and $O_{b,c}$–W^{VI}, respectively [26]. The hybrid sample HMS–HPA(V2) showed the bands of $H_5PMo_{10}V_2O_{40}$ with little shift in the DR-UV–vis spectra either before or after the reaction with O_2. These results indicate that $H_5PMo_{10}V_2O_{40}$ molecules were successfully immobilized on the HMS-NH_2 surface of HMS–HPA(V2) without collapse even after used for benzene oxidation. On the other hand, if the reactor was not charged with O_2, HMS–HPA(V2) showed a strong absorption band at about 740 nm after interacting with benzene and $Pd(OAc)_2$ at 393 K. The band at about 740 nm is a signal for the formation of the reduced species of heteropolyanions because this band can be assigned

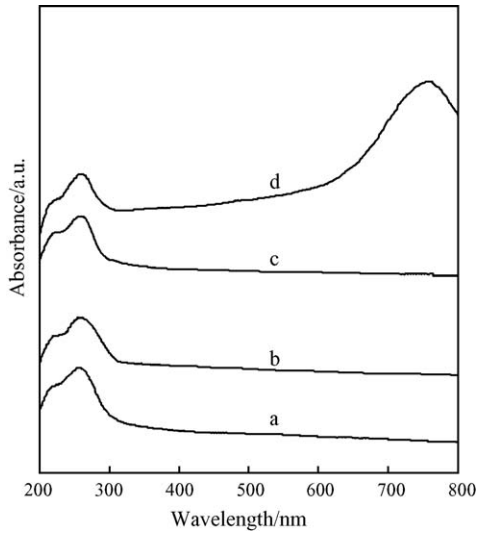

Fig. 7. UV–vis diffuse reflectance spectra of various samples: (A) $H_5PMo_{10}V_2O_{40}$ (HPA(V2)); (B) HMS–HPA(V2) before reaction; (C) HMS–HPA(V2) after reaction with O_2; (D) HMS–HPA(V2) after reaction without O_2.

to intervalence charge-transfer (IVCT) from $V^{IV}-O_b-V^V$ to $V^V-O_b-W^{IV}$ according to its strength and position [26]. Moreover, this band disappeared after introducing O_2 into the autoclave reactor. These results implied that heteropolyanions were reduced by palladium and/or benzene to form reduced species, which was re-oxidized by O_2. Thus, the system containing heteropolyanions and palladium could achieve catalytic oxidation of benzene using O_2 as an oxidant.

In the previous paper [28], we reported the epoxidation of propylene with O_2 in the presence of $Pd(OAc)_2$, peroxo-heteropoly compound and methanol, where $Pd(OAc)_2$ was reduced with methanol to form Pd^0 species, which was active for regenerating peroxo-heteropoly compound by O_2 for the propylene epoxidation. However, in this study, when we used methanol solvent for HPA + $Pd(OAc)_2$ or HMS–HPA + $Pd(OAc)_2$ systems, no phenol was formed and no Pd^0 species could be detected by the X-ray diffraction analyses of the used catalysts.

According to Refs. [11,29], the cycle of Pd^{2+} and Pd^{4+} plays an important role in the benzene oxidation to phenol by O_2 in the catalytic system consisting of $Pd(OAc)_2$, V-compound, HOAc, LiOAc and H_2O. Palladium acetate electrophilically attacks benzene molecule to give phenyl-palladium (II) acetate. Then the strong oxidant HPA oxidizes pheny-palladium (II) acetate to phenyl-palladium (IV) triacetate in the presence of HOAc and LiOAc. The formed phenyl-palladium (IV) triacetate undergoes reductive elimination to produce phenyl acetate, which is finally hydrated to form phenol. In a word, palladium is the active site for the benzene oxidation; heteropoly compound is the co-catalyst for re-oxidizing palladium to achieve the cycle of Pd^{2+} and Pd^{4+}. Because the reduced heteropoly compound could be oxidized by O_2, active Pd species is regenerated in situ and is achieved catalytic oxidation of benzene to phenol by O_2. The main byproducts are further oxidated products (catechol, hydroquinone, 1,4-benzoquinone) and oxidative coupling products (biphenyl). Because HPA and $Pd(OAc)_2$ dissolved in the mixed solvent easily diffuse in the reaction system, the homogeneous catalytic system showed higher benzene conversion than those obtained in the heterogeneous catalytic systems. The dual solid system showed very low yield of phenol since $H_5PMo_{10}V_2O_{40}$ molecules on HMS–HPA(V2) have few chance to re-oxidize $Pd(OAc)_2$ on HMS–$Pd(OAc)_2$ in the system. On the other hand, because both the heterogeneous catalytic systems and the homogeneous catalytic system possess the same active components and catalyze the benzene oxidation through the same reaction mechanism, the most effective heterogeneous system (HMS–HPA(V2) + $Pd(OAc)_2$) could obtain the same maximum achievable yield of phenol as that obtained over the homogeneous catalytic system (HPA + $Pd(OAc)_2$) by extending the reaction time or increasing the catalyst amount.

The dependences of benzene conversion and selectivity to phenol on the $Pd(OAc)_2$ amount in HMS–HPA(V2) + $Pd(OAc)_2$ catalytic system is shown in Fig. 8. The HMS–HPA(V2) amount was kept constant at 0.5 g. The catalytic system containing no $Pd(OAc)_2$ showed very low activity (0.8%) and did not form phenol at all, indicating that the coexistence of palladium and heteropoly compounds in the catalytic system is indispensable for improving the yield of phenol. When the amount of $Pd(OAc)_2$ increased from 0.005 to 0.03 g, the benzene conversion increased from 7.9 to 20.8% but the selectivity to phenol decreased from 81.1 to 56.0%. The oxidative coupling of benzene and the deep oxidation of phenol were promoted by the large amount of palladium.

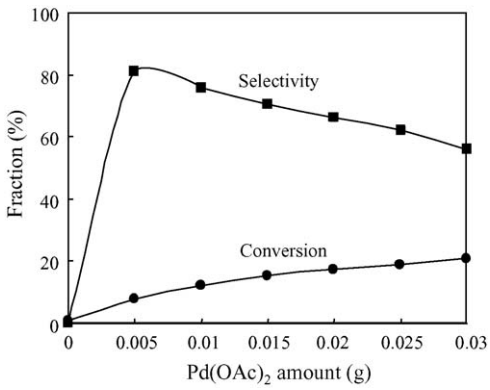

Fig. 8. Dependences of benzene conversion and selectivity to phenol on the $Pd(OAc)_2$ amount in HMS–HPA(V2) + $Pd(OAc)_2$ catalytic system for the benzene oxidation by O_2 at 393 K for 10 h. (●): benzene conversion; (■): selectivity to phenol. Autoclave, 50 ml; O_2, 2.0 MPa; HMS–HPA(V2), 0.5 g; LiOAc, 0.2 g; benzene, 2 ml; HOAc, 2 ml; H_2O, 4 ml; sulfolane, 2 ml; O_2, 2.0 MPa.

The effect of x in $H_{3+x}[PMo_{12-x}V_xO_{40}]$ ($x = 0$–3) in the heterogeneous system HMS–HPA + $Pd(OAc)_2$ is shown in Fig. 9. The conversions were 2.7, 10.6, 12.2 and 12.7%, and the selectivity to phenol were 59.8, 68.6, 75.6 and 72.4% for $x = 0$, 1, 2 and 3, respectively. The low activity of HMS–HPA(V0) + $Pd(OAc)_2$ implied that V sites in HPA are main active sites and Mo sites in HPA just possess a little catalytic ability for the benzene oxidation by O_2. The oxidation ability of Keggin structure heteropoly anion $[PMo_{12}O_{40}]$ increases by replacing the polyatom Mo by V, and decreases by replacing the polyatom Mo by W [24]. Thus, the oxidation ability of HPA is in the order of $H_3[PMo_{12}O_{40}] < H_4[PMo_{11}VO_{40}] < H_5[PMo_{10}V_2O_{40}] < H_6[PMo_9V_3O_{40}]$. Therefore, HMS–HPA(V3) + $Pd(OAc)_2$ catalytic system showed the highest benzene conversion for the benzene oxidation by O_2. However, because the selectivity to phenol in HMS–HPA(V3) + $Pd(OAc)_2$ was low due to the fur-

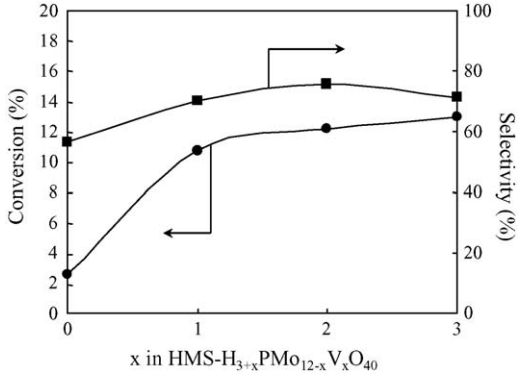

Fig. 9. Effect of x in HMS-$H_{3+x}PMo_{12-x}V_xO_{40}$ for the oxidation of benzene by O_2 over the heterogeneous catalytic system HMS–HPA + $Pd(OAc)_2$ at 393 K for 10 h. (●): benzene conversion; (■): selectivity to phenol. Autoclave, 50 ml; HMSHPA, 0.5 g; Pd(OAc)2, 0.01 g; LiOAc, 0.2 g; benzene, 2 ml; HOAc, 2 ml; H_2O, 4 ml; sulfolane, 2 ml; O_2, 2.0 MPa.

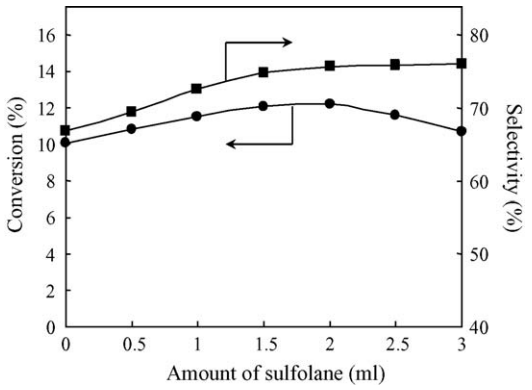

Fig. 10. Dependences of benzene conversion and selectivity to phenol on the sulfolane amount in the mixed solvent for the benzene oxidation by O_2 over heterogeneous catalytic system HMS–HPA(V2) + $Pd(OAc)_2$ at 393 K for 10 h. (●): benzene conversion; (■): selectivity to phenol. Autoclave, 50 ml; O_2, 2.0 MPa; HMS–HPA(V2), 0.5 g; $Pd(OAc)_2$, 0.01 g; LiOAc, 0.2 g; benzene, 2 ml; HOAc + H_2O + sulfolane = 8 ml; HOAc/H_2O = 1/2 (v/v).

ther oxidation of phenol, the highest yield of phenol was obtained at $x = 2$ in $H_{3+x}[PMo_{12-x}V_xO_{40}]$.

The effect of sulfolane in the mixed solvent for the oxidation of benzene by O_2 over the heterogeneous catalytic system HMS–HPA(V2) + $Pd(OAc)_2$ is shown in Fig. 10. Sulfolane is a solvent with high dipole moment (4.81 debye) and dielectric constant (43.26), thus showing the peculiar property in forming complexes with phenolic compounds [30]. Although the complex is not stable, it could prevent the further oxidation of phenol to some extent. It has been reported that sulfolane is effective for raising both the benzene conversion and the selectivity to phenol for the benzene oxidation over TS-1 by H_2O_2 [31]. As shown in Fig. 10, the selectivity to phenol increased with increasing amount of sulfolane and almost levelled off when the amount of sulfolane was more than 2 ml. On the other hand, the benzene conversion increased when the amount of sulfolane was less than 2 ml and vice versa. The highest yield of phenol was obtained when the amount of sulfolane was 2 ml.

In order to check whether $H_5[PMo_{10}V_2O_{40}]$ leaches from the surface of HMS or not in the heterogeneous catalytic system HMS–HPA(V2) + $Pd(OAc)_2$ for the benzene oxidation by O_2 at 393 K, we designed the following experiment. As shown in Fig. 11, after 0.5 g HMS–HPA(V2) and 0.01 g $Pd(OAc)_2$ were used as catalysts for the benzene oxidation by O_2 at 393 K for 10 h, the reaction was stopped and the solid catalyst HMS–HPA(V2) was recovered by filtration. Then the recovered HMS–HPA(V2) was put into another autoclave containing 0.01 g $Pd(OAc)_2$, 2 ml benzene and the mixed solvent. After it was charged with 2.0 MPa O_2, the second run was carried out for another 10 h at 393 K. In the meantime, the reaction liquid that filtrated out the solid catalyst HMS–HPA(V2) after the first run was also allowed to react for another 10 h at 393 K. As shown in Fig. 11, the solid catalyst HMS–HPA(V2) used for the second run showed no obvious reduction of the catalytic activity compared to the first run. On the other hand, the filtrate did not show any further reaction at 393 K for another 10 h. Moreover, the IR and XRD of the solid catalyst HMS–HPA(V2) did not show any changes after the reaction. These results indicate that the solid

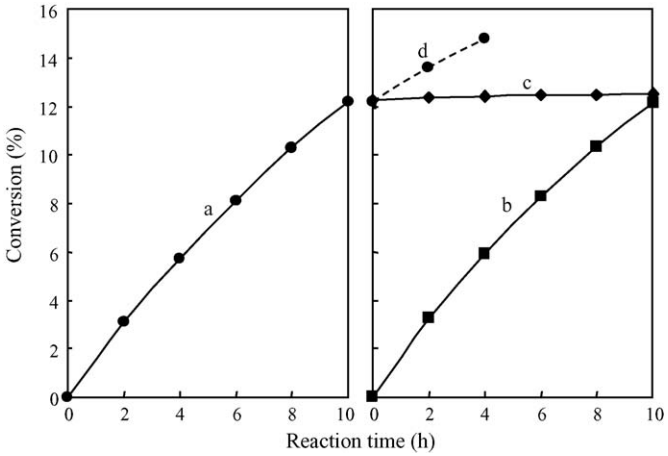

Fig. 11. Stability of heterogeneous catalytic system HMS–HPA(V2) + $Pd(OAc)_2$ for the benzene oxidation by O_2 at 393 K. (a) The first run, (b) the filtered solid catalyst HMS–HPA(V2) with new $Pd(OAc)_2$ for the second run, (c) the reaction of filtered solution after the first run filtered out the solid catalyst HMS–HPA(V2) and (d) the reaction of filtered solution after the first run with the solid catalyst HMS–HPA(V2).

catalyst HMS–HPA(V2) could be recycled by a simple filtration method and the active components (HPA) did not leach to the mixed solvent during the oxidation of benzene by O_2 at 393 K for 10 h.

The reusability of various heterogeneous catalytic systems containing solid catalysts for the oxidation of benzene by O_2 is shown in Fig. 12. After the reaction at 393 K for 10 h, the used solid catalysts were obtained by filtration. By adding the necessary reagents, the solid catalysts were reused for the benzene oxidation by O_2 at 393 K for another 10 h. The activity of HMS–HPA(V2) + $Pd(OAc)_2$ did not obviously decrease after HMS–HPA(V2) was used five times, implying HMS–HPA(V2) is a real heterogeneous catalyst without leaching active components to the mixed solvent during reaction [32]. In contrast, the catalytic system containing supported catalyst HPA(V2)/HMS and $Pd(OAc)_2$ showed a high benzene conversion (13.7%) for the first run but the benzene conversion rapidly decreased to 2.8% for the second run, which indicates that HPA leached from

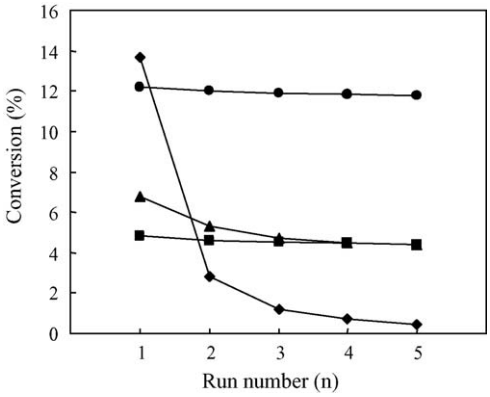

Fig. 12. Reusability of solid catalysts in various heterogeneous catalytic systems for the benzene oxidation by O_2 at 393 K for 10 h. (●): HMS–HPA(V2) + $Pd(OAc)_2$; (♦): HPA(V2)/HMS + $Pd(OAc)_2$; (▲): PIM–HPA(V2) + $Pd(OAc)_2$; (■): HPA(V2) + HMS–$Pd(OAc)_2$.

the surface of HMS and the oxidation of benzene took place in the homogeneous phase in the HPA(V2)/HMS + $Pd(OAc)_2$ system. As for PIM–HPA(V2) + $Pd(OAc)_2$ system, the activity decreased for the second and third runs but did not show further decrease for the forth and fifth runs. These results indicate that HPA molecules easily leach from PIM support before PIM–HPA(V2) was used for three runs and hardly leach thereafter. On the whole, the HMS immobilized HPA catalyst showed relatively high and sustained catalytic activity compared to the corresponding functional polymer immobilized HPA catalyst, which is similar to the catalytic characteristics of SBA-15 immobilized quaternary ammonium catalysts for the heterogeneous phase transfer reaction [33].

4. Conclusions

HPA and $Pd(OAc)_2$ were immobilized onto the functional organic groups grafted on the surfaces of HMS and PIM, and the resultant solid compounds were used as heterogeneous catalysts for the oxidation of benzene to phenol by O_2. The system containing HMS immobilized HPA and $Pd(OAc)_2$ (HMS–HPA + $Pd(OAc)_2$) is the most effective heterogeneous catalytic system in this study. Although the heterogeneous catalytic system HMS–HPA + $Pd(OAc)_2$ showed a lower activity compared to the homogeneous catalytic system HPA + $Pd(OAc)_2$, it achieved the same maximum yield of phenol as that obtained in the homogeneous catalytic system HPA + $Pd(OAc)_2$ by extending reaction time or increasing catalyst amount. Immobilizing HPA on HMS surface was more effective than immobilizing $Pd(OAc)_2$ on HMS surface. Moreover, the HMS immobilized HPA catalyst showed relatively high and sustained catalytic activity compared to the polymer PIM immobilized HPA catalyst. On the other hand, the dual solid system containing HMS–HPA(V2) and HMS–$Pd(OAc)_2$ showed a very low benzene conversion. As for the solvent effect, the selectivity to phenol could be improved by adding sulfolane to the reaction system, but the benzene conversion decreased when the mixed solvent contain high concentration of sulfolane. The solid catalyst HMS–HPA in the heterogeneous catalytic system HMS–HPA + $Pd(OAc)_2$ could be recovered by a simple filtration method and the active components (HPA) did not leach to the solvent during reaction.

Acknowledgement

We gratefully acknowledge the financial support from the Japan Society for the Promotion of Science (JSPS).

References

[1] B. Lücke, K.V. Narayana, A. Martin, K. Jähnisch, Adv. Synth. Catal. 346 (2004) 1407.
[2] M. Bonchio, V. Conte, F. Di Furia, G. Modena, S. Moro, J. Org. Chem. 59 (1994) 6262.
[3] G.I. Panov, A.K. Uriarte, M.A. Rodkin, V.I. Sobolev, Catal. Today 41 (1998) 365.
[4] W. Laufer, J.P.M. Niederer, W.F. Hoelderich, Adv. Synth. Catal. 344 (2002) 1084.
[5] M. Tani, T. Sakamoto, A. Mita, S. Sakaguchi, Y. Ishii, Angew. Chem. Int. Ed. 44 (2005) 2586.
[6] T. Kusakari, T. Sasaki, Y. Iwasawa, Chem. Commun. (2004) 992.
[7] S. Yamaguchi, S. Sumimoto, Y. Ichihashi, S. Nishiyama, S. Tsuruya, Ind. Eng. Chem. Res. 44 (2005) 1.
[8] Y. Liu, K. Murata, M. Inaba, Catal. Commun. 6 (2005) 679.
[9] T. Okuhara, N. Mizuno, M. Misono, Adv. Catal. 41 (1996) 113.
[10] N. Mizuno, M. Misono, Chem. Rev. 98 (1998) 199.
[11] L.C. Passoni, A.T. Cruz, R. Buffon, U. Schuchardt, J. Mol. Catal. A Chem. 120 (1997) 117.
[12] H.A. Burton, I.V. Kozhevnikov, J. Mol. Catal. A Chem. 185 (2002) 285.
[13] L.C. Passoni, F.J. Luna, M. Wallau, R. Buffon, U. Schuchardt, J. Mol. Catal. A Chem. 134 (1998) 229.
[14] T. Okuhara, Chem. Rev. 102 (2002) 3641.
[15] Y. Watanabe, K. Yamamoto, T. Tatsumi, J. Mol. Catal. A Chem. 145 (1999) 281.
[16] W. Kaleta, K. Nowinska, Chem. Commun. (2001) 535.
[17] N. Horita, M. Yoshimune, Y. Kamiya, T. Okuhara, Chem. Lett. 34 (2005) 1376.
[18] E.S. Pomarzanska, M. Hasik, W. Turek, A. Pron, J. Mol. Catal. A Chem. 114 (1996) 267.
[19] Y. Liu, K. Murata, M. Inaba, Green Chem. 6 (2004) 510.
[20] Y. Liu, K. Murata, M. Inaba, Chem. Commun. (2004) 582.
[21] S. Paul, J.H. Clark, Green Chem. 5 (2003) 635.
[22] L. Li, J. Shi, J. Yan, Chem. Commun. (2004) 1990.
[23] G.A. Tsigdinos, C.J. Hallada, Inorg. Chem. 7 (1968) 437.
[24] S. Paul, J.H. Clark, Green Chem. 5 (2003) 635.
[25] T. Pruβ, D.J. Macquarrie, J.H. Clark, J. Mol. Catal. A Chem. 211 (2004) 209.
[26] M.T. Pope, Heteropoly and Isopoly Oxometalates, Springer-Verlag, Berlin, 1983.
[27] K.S.W. Sing, D.H. Everett, R.A.W. Haul, L. Moscou, R.A. Pierotti, J. Rouquerol, T. Siemieniewska, Pure Appl. Chem. 57 (1985) 603.
[28] Y. Liu, K. Murata, M. Inaba, N. Mimura, Appl. Catal. B Environ. 58 (2005) 51.
[29] K. Murata, Y. Liu, M. Inaba, Catal. Lett. 102 (2005) 143.
[30] R.S. Drago, B. Wayland, R.L. Carlson, J. Am. Chem. Soc. 85 (1963) 3125.
[31] L. Balducci, D. Bianchi, R. Bortolo, R. D'Aloisio, M. Ricci, R. Tassinari, R. Ungarelli, Angew. Chem. Int. Ed. 42 (2003) 4937.
[32] R.A. Sheldon, M. Wallau, I.W.C.E. Arends, U. Schuchardt, Acc. Chem. Res. 31 (1998) 485.
[33] L. Li, J. Shi, J. Yan, H. Chen, X. Zhao, J. Mol. Catal. A Chem. 209 (2004) 227.